



A Pixel-Isolated Flexible Liquid Crystal Display with a Homogeneous Alignment on an Amorphous ZrO₂ Thin Film

Young-Hwan Kim,^a Byoung-Yong Kim,^a Hong-Gyu Park,^a Jae-Hong Kwon,^b
Kyeong-Kap Paek,^c Byeong-Kwon Ju,^{d,z} and Dae-Shik Seo^{a,*}

^aInformation Display Device Laboratory, School of Electrical and Electronic Engineering, Yonsei University, Seoul 120-749, Korea

^bSamsung Electronics Corporation Limited, System LSI Division, Foundry Business Team, SRAM and Design Group, Yongin, Gyeonggi 446-711, Republic of Korea

^cDepartment of Electronic Engineering, Daejin University, Pocheon, Gyeonggi 487-711, Korea

^dDisplay and Nanosystem Laboratory, College of Engineering, Korea University, Seoul 136-701, Korea

In this study, we developed a pixel-isolated flexible liquid crystal display (LCD) with a homogeneous alignment on inorganic thin-film surfaces using ion beam (IB) irradiation. The amorphous ZrO₂ (a-ZrO₂) film, used as a homogeneous alignment layer on the plastic substrate, was deposited at room temperature. Pixel walls based on poly(dimethylsiloxane) were fabricated using a simple photolithographic process. Even under external tension, the two plastic substrates remained tightly attached by the pixel walls at each pixel; the highly uniform alignment of liquid crystals was optimized on the a-ZrO₂ surface. The electro-optical performance of our flexible device was highly reliable and comparable to that of conventional glass-substrate LCDs.
© 2010 The Electrochemical Society. [DOI: 10.1149/1.3492409] All rights reserved.

Manuscript submitted April 30, 2010; revised manuscript received September 2, 2010. Published September 27, 2010.

The development of paperlike electronic displays has been focused on flexible applications because they have the potential to open up not only smart cards, the center fascia of cars, and display systems for other designs but also future application areas including wearable computers. Recently, many research groups have successfully demonstrated active-matrix (AM) organic light emitting diodes.¹⁻⁷ Simultaneously, organic thin film transistor (TFT)-driven AM liquid crystal displays (LCDs), including polymer-dispersed LCDs, twisted nematic (TN), cholesteric, and bistable ferroelectric liquid crystal (LC) modes, have been proposed for use in flexible displays to enhance mechanical stability and electro-optical (EO) performance (i.e., fast response time, low voltage-driven).²⁻⁸ However, they have some critical problems related to the passivation and alignment layers; rubbing and high temperature processes can still be encountered when fabricating commercial flexible displays and in integrating an active element (e.g., OTFT, poly-Si TFT).¹⁻⁸ Thus, new technologies that are simple and applicable at low temperatures need to be developed for practical applications.

Two key requirements need to be satisfied and resolved during fabrication. The first is to fabricate a uniform and stable alignment of the LC molecules with good electrical performance and stability.⁸⁻¹¹ The second is to simplify the process by substituting the multilayers for an alignment layer of the LC molecules and passivation layers of the TFT to integrate the TFT.⁵⁻⁷ However, a monolayer substituting the multilayers has not yet been developed. In the present study, we developed pixel-isolated TN-LCDs fabricated on a flexible amorphous ZrO₂ (a-ZrO₂) thin film. This inorganic monolayer has the capability to stably align the LC molecules and to encapsulate the organic and inorganic layers against air damage.⁵

Previously, we have reported that a pixel-isolated flexible liquid crystal display (PIF-LCD) fabricated on a polyimide (PI) surface using ion beam (IB) irradiation and an a-ZrO₂ film deposited using an electron-beam (E-beam) evaporator at room temperature was examined as a dielectric passivation for OTFT.^{5,7} In this study, we developed flexible a-ZrO₂ as a homogeneous alignment layer using IB irradiation. Our concept of aligning the LC molecules and spontaneously encapsulating the TFT against ambient moisture and oxygen without additional multilayers is depicted in Fig. 1a. The a-ZrO₂ thin film produces a TFT passivation insulator simultaneously with the alignment of the LC molecules. Moreover, from the scientific viewpoint, the anisotropic interactions between the LC molecules

and the flexible a-ZrO₂ surfaces are important to the understanding of the interfacial phenomena of soft matter. Using this approach, our PIF-LCDs have a response time of ~10 ms, resulting in a highly reliable EO performance in the bent state, comparable to that of glass-substrate LCDs.

Figure 1a illustrates our PIF-LCD with the multifunctional a-ZrO₂ substrate used as an alignment layer of LC molecules and a TFT passivation layer. The a-ZrO₂ films (1000 Å thick) were evaporated on an indium tin oxide-coated glass substrate using E-beam evaporation at an average deposition rate of 2 Å/s at room temperature. A stepper motor that rotated the substrate during the film deposition drove the substrate holder. We used a photolithographic process to fabricate the PDMS pixel walls; the fabricated PDMS pixel walls on a-ZrO₂ are depicted in Fig. 1b.⁸ As shown in the scanning electron microscopy images of Fig. 1c, the PDMS pixel walls of the top substrate were clearly attached after external bending. The a-ZrO₂ thin films were then irradiated with Ar⁺ IB plasma in the range 600–2400 eV per 600 eV using a DuoPIGatron-type IB system. The IB incident angles were 45° and the exposure time was 60 s for all samples. The IB system used in this study was based on a DuoPIGatron ion source.⁸⁻¹² The substrates were fabricated in an antiparallel configuration with a cell gap of 60 μm to allow for the observation of the pretilt angles with microphotographs. Additionally, TN-LCDs were prepared with a cell gap of 5 μm to allow for the examination of the voltage–transmittance characteristics. A positive LC ($T_C = 72^\circ\text{C}$, $\Delta\epsilon = 8.2$, $\Delta n = 0.077$) was then injected into the cell. Finally, two fabricated flexible substrates were aligned antiparallel for the TN-LCDs and bonded together using our PDMS pixel wall-based IB irradiation method at room temperature.

We used X-ray photoelectron spectroscopy (XPS), X-ray diffraction (XRD), atomic force microscopy (AFM), and contact angle measurements to investigate the chemical and physical mechanisms of the intermolecular chemical reaction between the a-ZrO₂ and the LC molecules caused by the IB irradiation. Some inorganic films have various phases, depending on the deposition process or the IB irradiation.¹³⁻¹⁵ Therefore, it is important to determine the phase via XRD patterns, which reveal the crystallinity and orientation under different deposition conditions.⁹⁻¹¹ Using AFM and XRD, we investigated the transitions in the morphology and the crystallinity of the a-ZrO₂ thin-film characteristics before and after IB irradiation. As shown in Fig. 2, all the peaks corresponded well to the silicon (100) structure when compared with the images from the standard XRD database. No other peaks corresponding to ZrO₂ were observed in the data, suggesting that the deposited ZrO₂ was present in an amorphous phase.

* Electrochemical Society Active Member.

^z E-mail: bkju@korea.ac.kr; dsseo@yonsei.ac.kr

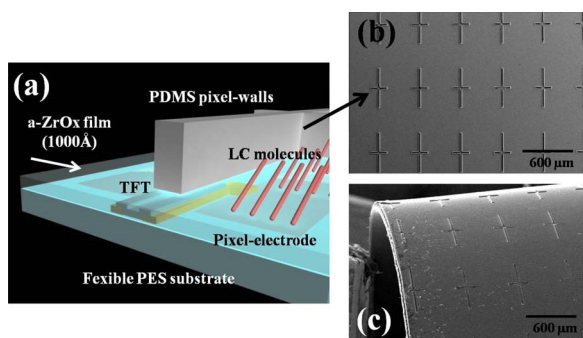


Figure 1. (Color online) The schematic illustration of our PIF-LCD with the multifunctional a-ZrO₂ substrate used as an alignment layer for the LC molecules and a passivation layer for TFTs.

The AFM investigation was also performed to elucidate effects on the behavior of the LC alignment. The root-mean-square (rms) roughness values of the IB-irradiated ZrO film surface as a function of the IB intensity under the same conditions are shown in Fig. 2 insets. The rms roughness slightly changed from 2.5 to 2.6 nm. These results reveal that no surface transformation induced IB bombardment at the 1800 eV IB intensity was seen. Consequently, no morphology effect indicating an LC alignment was directly related, whereas the amorphous network near the IB-irradiated surfaces dominantly affects the LC alignment and the pretilt angle.⁹⁻¹⁵

Figure 3a-c shows the relationship between the XPS spectra and the surface energy before and after the IB exposure. The contact angle and the XPS of each ZrO₂ film were measured before and after the IB irradiation at 2400 eV, 45°, and 60 s. Before the XPS analysis, all of the binding energies were adjusted from the C 1s peak at 285.0 eV.¹⁶ As shown in Fig. 3a, the XPS spectra for the O 1s peaks resolved into two components and the full width at half-maximum values of the O 1s bonds were ~1.5 eV. The area ratio was also constant for all spectra. The binding energy peak located at 529.5 ± 0.5 eV is from surface contamination, namely OH⁻.¹⁶ Regarding the O-Zr peak, the lowest amplitude was optimized after the IB irradiation at 2400 eV. As shown in Fig. 3b, the Zr 3d peaks before the IB irradiation were centered at 182.5 and 184.8 eV. The IB irradiation of 2400 eV, which can induce LC alignment, shifted the Zr 3d peaks to lower energy peaks, 182.2 and 184.6 eV, which represent an oxygen deficiency (i.e., Zr⁰). The binding energy of the oxygen deficiency is higher than that of the fully oxidized metal oxide (i.e., Zr⁴⁺). This result indicated that ZrO₂ had been converted to ZrO_{x<2} by the IB irradiation.¹⁶

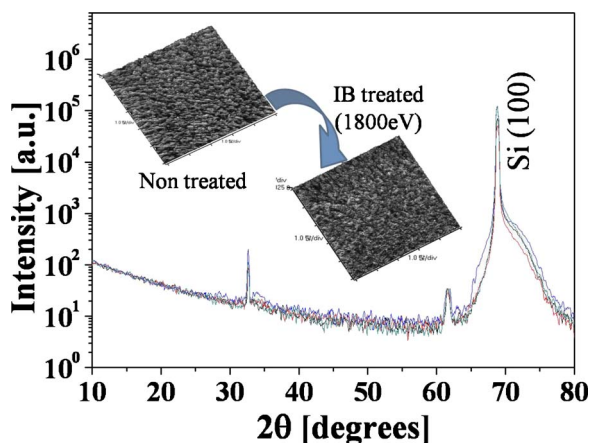


Figure 2. (Color online) The XRD spectra and AFM images of the a-ZrO₂ film on a (100) silicon substrate before and after IB irradiation.

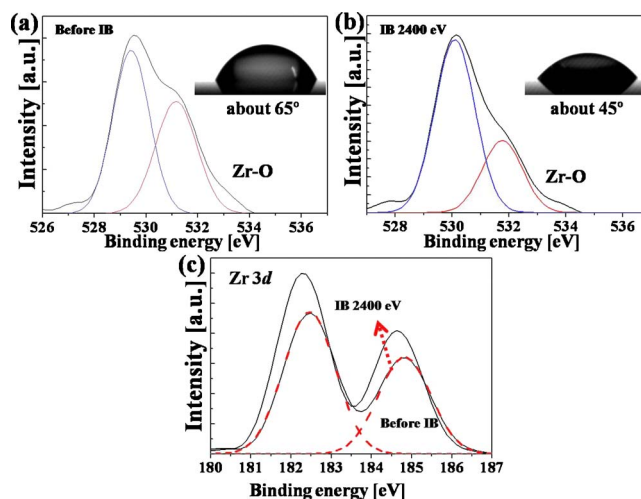


Figure 3. (Color online) The curve fit of the XPS spectra for the O 1s and Zr 3d peaks from the a-ZrO₂ surface and the contact angle (a) before and (b) after an IB irradiation at 2400 eV. These results show the intensity of the Zr-O bonding as a function of the IB irradiation. (c) The Zr 3d peaks from the a-ZrO₂ with an IB energy of 0 and 2400 eV.

The contact angle on a-ZrO_x films is shown as a function of IB intensity in Fig. 4. This may induce the activation of the ZrO₂ film surface; thus, the contact angle on Zr⁰ after the IB irradiation is lower than that of the fully oxidized Zr⁴⁺.^{10-12,16} The measured pretilt angles had a high degree of error at low intensity energies of 600 and 1200 eV due to random LC orientation (see Fig. 4 insets). When the intensity of the IB energy was up to 1800 eV, LC molecules are uniformly aligned and the value of pretilt angles was fixed at ~0.5°. In this experiment, pretilt angles were measured using the crystal rotation method (TBA 107 device, Autronic).^{10,11}

As a result of surface analysis, the activated amorphous network that had large polarizability was attributed to a stronger π-π interaction with the LC molecules. Thus, the formation of the pretilt angle was attributed to the surface energy by breaking the ZrO_{x<2} according to the intensity of the IB, whereas a preferential orientation of LC molecules depended on the IB direction. Through this physical phenomenon, we optimized the LC molecule alignment on the a-ZrO₂.

Finally, a typical 6 × 6 cm flexible LCD was fabricated with a crossed polarizer using an applied voltage of 5 V (Fig. 5). A test of the mechanical stability and reproducibility of the flexible LCD was

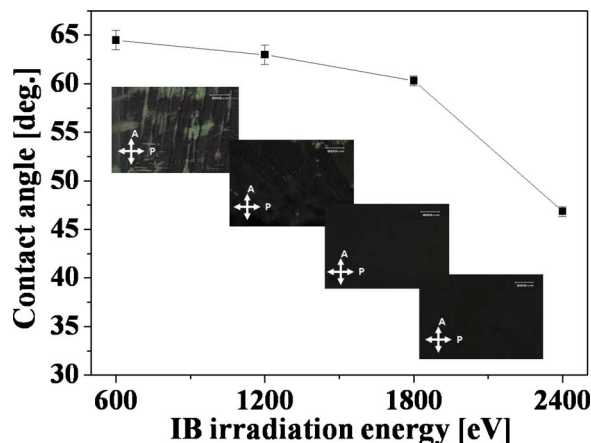


Figure 4. (Color online) The comparison of the contact angle results in terms of the LC alignment under the same IB intensity.

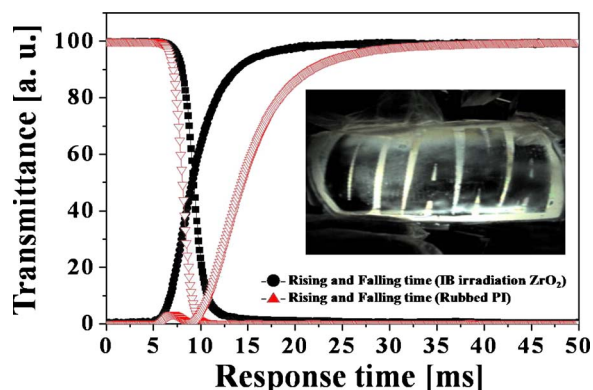


Figure 5. (Color online) The EO transmission and response of the PIF-LC cell. The measured rise and fall times, defined as the transition times between 90 and 10% EO transmittance, were $\tau_r = 2.7$ ms and $\tau_f = 7.1$ ms, respectively. Inset: A photomicrograph of a prototype PIF-LCD panel displays the logo “DIANA” at 5 V under extreme deformation.

conducted with an $R < 10$ mm, expressed as a geometrical curvature radius on a translation stage.⁸ The EO performance of the flexible LCDs is also exhibited by examining the transmission of light through two TN test panels as a function of the voltage applied across the cell.⁸ The cell spacing was ~ 5 μm . Our flexible cell and a conventional glass cell containing PI film were compared using dynamic EO response. The measured rise (τ_r) and fall (τ_f) times were 2.7 and 7.1 ms, respectively. The τ_r for our flexible LCD was notably faster than that of the other flexible display fabricated with the imprinted microgroove or even the conventional PI alignment layer.⁸ This difference can be attributed to the different characteristics of the high- k ZrO_2 and conventional PI alignment layers.^{10,11} This leads to the conclusion that with a reduced threshold voltage, LCDs can operate effectively at lower voltages and decreased power.

In this study, we developed flexible LCDs with a homogeneous alignment on a- ZrO_2 using IB irradiation and demonstrated how to

produce a homogeneous alignment of LCs on a- ZrO_2 . Such LCDs could be manufactured at a lower cost than is associated with devices produced by multilayering (i.e., an alignment layer, an overcoat layer, and a TFT passivation layer), especially when used for the production of large, high resolution LCDs. It is believed that our new concept produces flexible LCDs that are more reliable than other flexible displays. The film has great potential as a thin and transparent barrier layer for TFTs and future flexible display applications; such experiments will be the subject of future work.

Yonsei University assisted in meeting the publication costs of this article.

References

1. A. Koudymov, C. X. Wang, V. Adivarahan, J. Yang, G. Simin, and M. A. Khan, *IEEE Electron Device Lett.*, **28**, 5 (2007).
2. J. A. Rogers, Z. Bao, K. Baldwin, A. Dodabalapur, B. Crone, V. R. Raju, V. Kuck, H. Katz, K. Amundson, J. Ewing, et al., *Proc. Natl. Acad. Sci. U.S.A.*, **98**, 4835 (2001).
3. P. Mach, S. J. Rodriguez, R. Nortup, P. Wiltzius, and J. A. Rogers, *Appl. Phys. Lett.*, **78**, 3592 (2001).
4. C. D. Sheraw, L. Zhou, J. R. Huang, D. J. Gundlach, T. N. Jackson, M. G. Kane, I. G. Hill, M. S. Hammond, J. Campi, B. K. Greening, et al., *Appl. Phys. Lett.*, **80**, 1088 (2002).
5. N.-R. Kim, Y.-D. Lee, K.-K. Paek, J.-W. Lee, J.-K. Kim, S.-W. Hwang, and B.-K. Ju, *Surf. Interface Anal.*, **39**, 64 (2007).
6. Y.-H. Kim, J.-H. Kwon, S.-I. Shin, B.-Y. Oh, H.-G. Park, K.-K. Paek, B.-K. Ju, and D.-S. Seo, *Electrochem. Solid-State Lett.*, **12**, H305 (2009).
7. J.-M. Kim, J.-W. Lee, J.-K. Kim, B.-K. Ju, J.-S. Kim, Y.-H. Lee, and M.-H. Oh, *Appl. Phys. Lett.*, **85**, 6368 (2004).
8. Y.-H. Kim, H.-G. Park, B.-Y. Oh, B.-Y. Kim, K.-K. Paek, and D.-S. Seo, *J. Electrochem. Soc.*, **155**, J371 (2008).
9. J.-B. Kim, K.-C. Kim, H.-J. Ahn, B.-H. Hwang, D.-C. Hyun, and H.-K. Baik, *Appl. Phys. Lett.*, **90**, 043515 (2007).
10. W.-K. Lee, B.-Y. Oh, J.-H. Lim, H.-G. Park, B.-Y. Kim, H.-J. Na, and D.-S. Seo, *Appl. Phys. Lett.*, **94**, 223507 (2009).
11. H.-G. Park, Y.-H. Kim, B.-Y. Oh, W.-K. Lee, D.-S. Seo, and J.-Y. Hwang, *Appl. Phys. Lett.*, **93**, 233507 (2008).
12. J.-H. Lim, Y.-H. Kim, B.-Y. Oh, B.-Y. Kim, J.-M. Han, J.-Y. Hwang, and D.-S. Seo, *Proc. SPIE*, **7404**, 74040X (2010).
13. P. Karmakar, S. A. Mollick, D. Ghose, and A. Chakrabarti, *Appl. Phys. Lett.*, **93**, 103102 (2008).
14. B.-Y. Oh, W.-K. Lee, Y.-H. Kim, and D.-S. Seo, *J. Appl. Phys.*, **105**, 054506 (2009).
15. M. Lu, *Jpn. J. Appl. Phys., Part 1*, **43**, 8156 (2004).
16. C. Morant, J. M. Sanz, L. Galan, L. Soriano, and F. Rueda, *Surf. Sci.*, **218**, 331 (1989).